Effects of Pulse Shaping in Laser Spectroscopy and Nuclear Magnetic Resonance

WARREN S. WARREN

Pulsed excitation fields are routinely used in most laser and nuclear magnetic resonance (NMR) experiments. In the NMR case, constant amplitude (rectangular) pulses have traditionally been used; in laser spectroscopy the exact pulse shape is often unknown or changes from shot to shot. This article is an overview of the effects of radio-frequency and laser pulse shapes and the instrumental requirements for pulse shaping. NMR applications to selective excitation, solvent suppression, elimination of phase roll, and reduced power dissipation are discussed, as are optical applications to soliton generation, velocity selective excitation, and quantitative population transfer.

MY INTENTION IS TO GIVE A BRIEF OVERVIEW OF THE uses of shaped pulses to reduce experimental difficulties in both NMR and laser spectroscopy. Analogous experiments are done in both of these fields; superficially, they seem very different, but they have strong mathematical similarities. The idea of using enhanced control over the radiation field to simplify spectroscopic measurements is not new; sequences of "rectangular" (constant amplitude) radio-frequency (RF) pulses with adjustable delays and phase shifts have played a central role in the development of NMR spectroscopy. Commercially available NMR spectrometers switched a decade ago from continuous to pulsed irradiation primarily because of sensitivity, but of equal practical importance was the opportunity this provided for research groups not specializing in NMR spectroscopy to apply extremely sophisticated sequences in a variety of applications in molecular biology, chemistry, and solid-state physics. Even after 40 years of development of multiple pulse spectroscopy, however, some NMR experiments remain fundamentally difficult:

1) It is often advantageous to give weak, narrow bandwidth pulses as part of a longer sequence to reduce data acquisition time or to enhance sensitivity. As an example, in "two-dimensional" (2D) NMR pulse sequences, the magnetization after the final pulse is measured for an extended period (giving a free induction decay, or FID), and also recorded as a function of one interpulse delay to give a matrix of data points (*1*). Broadband pulses generally force measurement of separate FIDs from a large number N of different interpulse delays to achieve acceptable frequency resolution (N is the ratio of the spectral width to the needed frequency resolution). However, if only a small portion of the spectrum in that dimension is interesting (for example, the amide region), then selective pulses dramatically decrease N, and hence decrease the time needed to acquire a usable spectrum. Unfortunately, long rectangular pulses still excite substantial magnetization outside of the nominal bandwidth. The discontinuities at the beginning and the end of the pulse produce high-frequency components in the excitation, thus spoiling the selectivity.

2) Solvent suppression is often crucial to prevent dynamic range overload of the receiver in biological applications, or to produce acceptable sensitivity. Most common solvent suppression sequences remove the water peak only at the expense of enormous phase and amplitude distortions in the excited peaks. These distortions can often be corrected in a simple FID, but correction is impossible in 2D or other sophisticated experiments.

3) High power amplifiers are needed for solid-state experiments, and probe arcing or sample heating can be a problem.

The many successful applications of complex NMR pulse sequences stand in stark contrast to developments in optical coherent transient spectroscopy. The most common laser-pulse sequences (*2*)—two-pulse photon echoes, stimulated echoes, and transient gratings—do not require specific pulse shapes or bandwidths [even "incoherent pulses" have been used (*3*)] and are unaffected by phase shifting of the individual pulses in the sequence. This insensitivity is experimentally convenient, but the information content is far less than can be found through the subtle manipulations of molecular interactions now commonplace in NMR. Phases are important for three-pulse echoes (*4*), composite pulses (*5*), and photon-locking sequences (*6, 7*), which have so far been demonstrated only on a

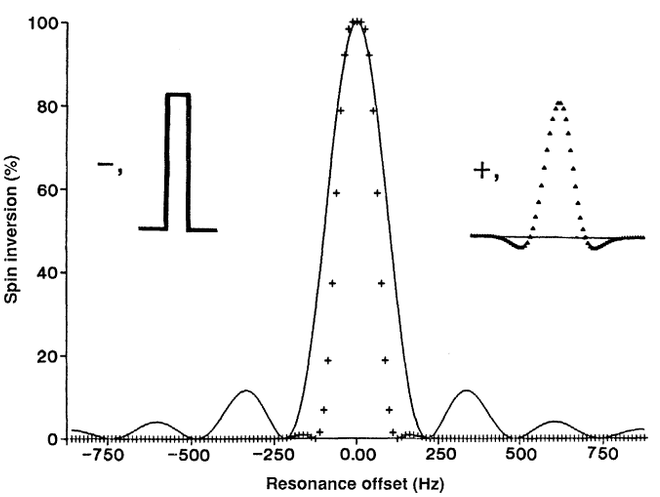

Fig. 1. Inversion profiles for (——) a rectangular π pulse and (+++) a Hermite-shaped pulse as a function of resonance offset (the difference between exact spin resonance and the pulse carrier wave frequency). Notice that the effects of the rectangular pulse are neither localized nor uniform, which leads to enhanced power dissipation and poor selectivity. [Reprinted with permission from *Journal of Magnetic Resonance* (*19*)]

The author is in the Department of Chemistry, Princeton University, Princeton, NJ 08544.

nanosecond time scale. The use of two picosecond pulses with variable interpulse phase shifts can eliminate fluorescence (*8*) or enhance frequency doubling efficiency (*9*). Theoretical work has shown that phase-shifted pulse sequences can enhance multiphoton pumping (*10*) or measure contributions from transition electric dipole-dipole interactions in condensed phases (*11*).

Analogs of more sophisticated NMR sequences would certainly be quite useful in optical spectroscopy, but these techniques rely on the inherent simplicity of spin systems. Phrased in the language of optical spectroscopists, all proton spin flips have the same dipole moment, all samples are optically thin and exhibit no propagation effects, NMR transmitters are perfectly stable monochromatic radiation sources, and the entire proton NMR spectrum has a small bandwidth. None of these assumptions is generally true for laser spectroscopy. The ability to selectively excite a single transition or part of a transition frequently becomes important, as does the ability to correct for laser imperfections and spectral complexity.

Pulse shape effects have been discussed much more quantitatively and extensively in a recent review article (*12*). The theoretical formalisms can be complicated and are still incomplete. This field is still rapidly evolving, particularly in applications to solids or coupled spins. Nonetheless, pulse shaping is readily implemented on well-designed commercial NMR spectrometers; programmable laser-pulse shaping with 100-fs resolution is possible; and virtually every pulse sequence can be executed with reduced power, better reproducibility, and fewer artifacts if some nonrectangular shape is used. In this article I concentrate on only a few straightforward and well-understood applications, discuss how pulse shaping is implemented, and show the general applicability of the technique.

General Effects of Shaped Pulses

It is easy to become spoiled by the theoretical sophistication of NMR spectroscopy. The last decade has seen examples of repeated 64-pulse line-narrowing sequences, 125-pulse composite-pulse sequences, and 4096-pulse multiple quantum sequences (*1*). In each case the theory was sufficiently good that initial disagreement between theory and experiment implied that the spectrometer was misaligned; when the spectrometer worked correctly, theory and experiment agreed.

Pulse shaping is different. Qualitative statements are easy: the excitation profile from an RF or laser pulse depends critically on the pulse shape, since changing the shape changes the magnitudes of the frequency components. If the pulse is extremely weak, linear response holds. In a two-level system (energies E_1 and E_2), the resonance frequency ω_0 equals $(E_2 - E_1)/\hbar$ (where $\hbar$ is Planck's constant divided by 2π); the induced magnetization (or optical polarization) is proportional to the amplitude of the magnetic field (or electric field) component at frequency ω_0; and the excited population is proportional to the square of this amplitude. But more intense pulses generate an enormously more complex response. For example, the effects of a rectangular pulse have been understood for half a century (*13*). The amplitude is conventionally expressed in units of the "Rabi frequency" ω_1, which equals $\gamma B_1/\hbar$ (γ is the gyromagnetic ratio and B_1 is the RF field strength) for NMR or $(\mu \cdot \mathbf{E})/\hbar$ for an optical two-level system (μ is the transition dipole moment vector and $\mathbf{E}$ is the electric field vector). The maximum polarization or transverse magnetization is generated if the pulse carrier wave is exactly resonant with the transition frequency and the pulse length T is such that $\omega_1 T = \pi/2$. Doubling the pulse length makes $\omega_1 T = \pi$, and population is transferred completely between the two levels (100% inversion). Most NMR and optical pulse sequences use these "$\pi/2$ pulses" or "π pulses" for maximum signal.

Off-resonance effects can also be readily calculated; Fig. 1 shows the inversion for a rectangular π pulse. The basic problem with selective excitation is apparent since the profile is neither uniform nor well localized. If the pulse length is doubled yet again, the "2π pulse" returns all spins on resonance to their initial states.

Unfortunately, this rectangular pulse case is the *only one* that has been solved for all initial conditions, all resonance offsets, and all amplitudes. The only other nearly complete solution to date (*14*) (all resonance offsets and all amplitudes, starting from equilibrium) is for the pulse shape $(\text{sech}\ \alpha T)^{1+\mu i}$. This complex function is shown in Fig. 2; the real part should be viewed as multiplying a cosine wave and the imaginary part as multiplying a sine wave. The waveform can also be written as a hyperbolic secant envelope with a hyperbolic tangent frequency sweep. The effects of this pulse differ dramatically from the rectangular pulse case (Fig. 3) (*15*). The inversion profile is rectangular, and is essentially unaffected both theoretically and experimentally when the peak power is varied by two orders of magnitude.

The usefulness of this shape in NMR is limited because it does not work as an echo pulse. However, it is tremendously useful as a laser

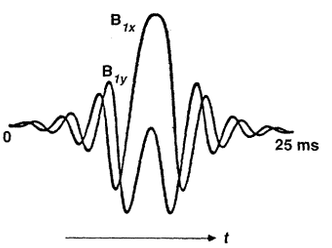

Fig. 2. Real and imaginary parts of the envelope $(\text{sech}\ \alpha T)^{1+5i}$. The real part can be viewed as modulating a cosine wave, and the imaginary part as multiplying a sine wave. This waveform looks very complicated, but commercially available circuit boards give 2048 point approximations to any shape, so such a shape is not difficult to implement. This is the only pulse shape more complicated than a rectangular pulse for which a nearly complete analytic solution has been performed.

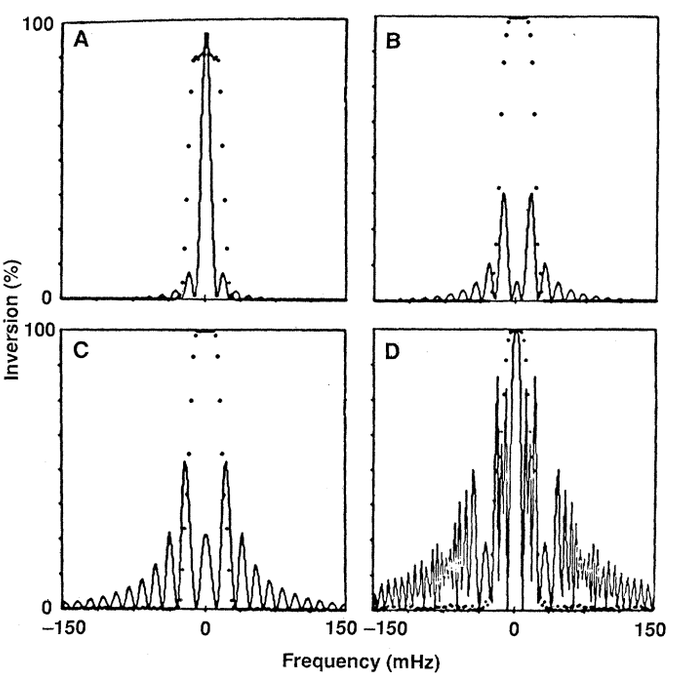

Fig. 3. Inversion profiles for (——) rectangular and (···) $(\text{sech}\ \alpha T)^{1+5i}$ pulses for pulse amplitudes of (**A**) 1×, (**B**) 4×, (**C**) 16×, and (**D**) 64× peak power. Most NMR spectroscopists' "intuition" about pulse sequence effects is based on the magnetization rotations induced by rectangular pulses, but the obvious insensitivity to amplitude variations and the uniform excitation profile for $(\text{sech}\ \alpha T)^{1+5i}$ make this intuition generally useless for shaped-pulse sequences. [Adapted from (*15*); reprinted with permission from *The Proceedings of the Society for Photo-Optical Instrumentation and Engineering*]

pulse, because it generates complete inversions even if $\mu \cdot \mathbf{E}$ varies (because of laser amplitude jitter, the transverse electric field distribution, overlapping lines, or different spatial directions of μ). We have applied 100-ns versions of this shape as a laser pulse to excite a single velocity component in a Doppler-broadened gas (*16*). This experiment permits direct measurement of velocity-changing collision probabilities.

The gross differences in Fig. 3 suggest that understanding even the qualitative effects of changing pulse shapes is difficult, and this is in fact true. The excitation profile resembles the Fourier transform of the pulse shape only if the pulse area is very small. For example,

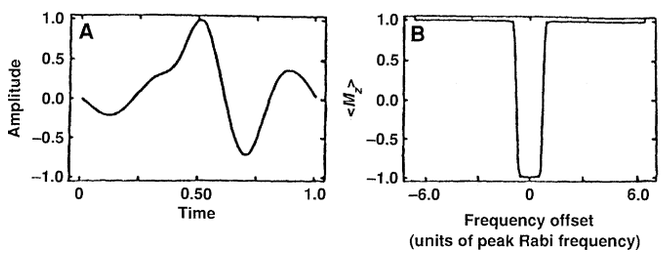

Fig. 4. (**A**) Asymmetric pulse shape optimized for a highly rectangular inversion profile. (**B**) Calculated inversion profile.

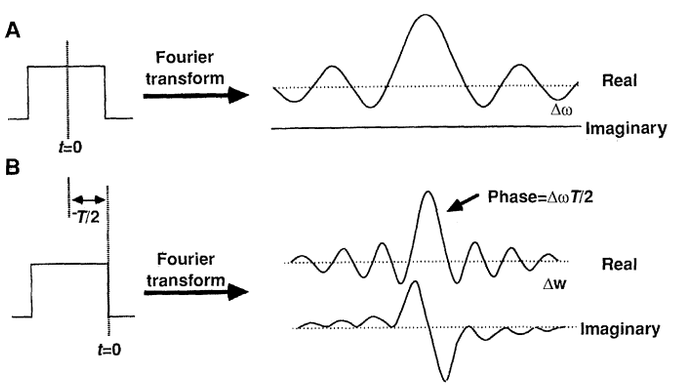

Fig. 5. Phase roll is a simple consequence of linear response theory; it is also present in spectra excited by most simple pulse shapes. (**A**) Near resonance, all transitions are in phase (the Fourier transform is real and positive). (**B**) Detection that begins after the pulse does not give all transitions in phase. Phase roll is approximately linear, but this does not hold for overlapping lines. [Adapted from (*31*); reprinted with permission from *Journal of Magnetic Resonance*]

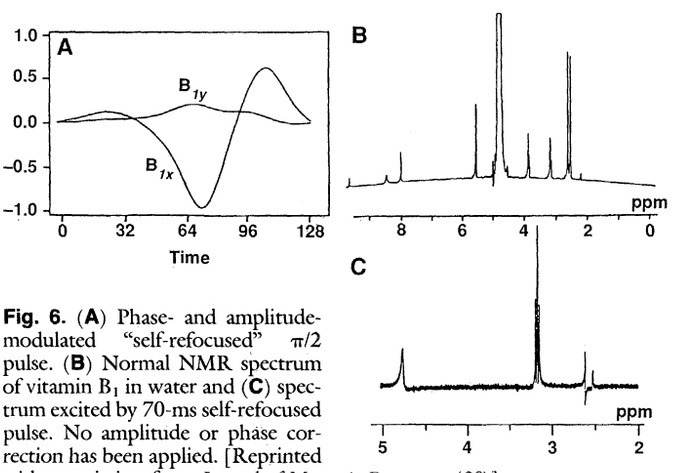

Fig. 6. (**A**) Phase- and amplitude-modulated "self-refocused" $\pi/2$ pulse. (**B**) Normal NMR spectrum of vitamin B_1 in water and (**C**) spectrum excited by 70-ms self-refocused pulse. No amplitude or phase correction has been applied. [Reprinted with permission from *Journal of Magnetic Resonance* (*28*)]

a $(\sin \alpha t)/t$ envelope (t is time) has a rectangular Fourier transform, and such a pulse with area $<\pi/6$ partially excites a rectangular distribution. But distortions are apparent if the area is increased to $\pi/2$, and the inversion profile from a π pulse is highly nonrectangular. Even more counterintuitive is the recent discovery that an infinitely large number of very different amplitude-modulated pulse envelopes, when raised to the $(1 + \mu i)$ power, all give rectangular and amplitude-insensitive inversion profiles (*17*); this unusual complex function plays a special role in the inverse scattering reformulation of the Bloch equations (*18*).

Perturbative expansions can describe simple amplitude-modulated shapes (*19*), such as the "Hermite pulse" in Fig. 1. This pulse is extremely simple and its Fourier transform is not very rectangular, yet it generates a clean and uniform excitation profile. Computerized optimization methods are more generally applicable, and results published by several different groups (*20, 21*) show that many different pulse shapes give nearly (or even exactly) the same inversion profile. The effects of any pulse shape can be formally calculated by breaking it up into a large number of small, nearly constant pieces, and the amplitudes of the waveform or of its Fourier transform can be systematically varied. This approach has produced some remarkably useful shapes. One of our asymmetric amplitude-modulated π pulses is shown in Fig. 4 (*22*); Murdoch, Lent, and Kritzer (*20*) also list many other shapes in their recent paper. It is particularly true for π pulses that the Fourier transform gives little clue as to the selectivity; a shape like this one is difficult to predict or understand from first principles, so the optimization gives little insight as to why it works so well. However, computer-optimized shapes work experimentally as well as theoretically, and are used clinically in many hospitals for enhanced resolution in magnetic resonance images.

Spectroscopic Applications of Specific Pulse Shapes

π Pulses. There is no "best pulse shape." The best choice for a particular application depends on trade-offs between such factors as the need for uniform excitation, for localized effects, or for the narrowest possible bandwidth. Table 1 illustrates these trade-offs for a number of different amplitude-modulated π pulse shapes; in each case the same peak power is assumed. These pulse shapes can also be used as echo pulses.

If all that is desired is partial excitation over a broad range of frequencies, a rectangular pulse is not a bad choice. However, the completely inverted region is quite small, which is why commercial NMR spectrometers must give <20 μs π pulses ($\omega_1 \approx 2\pi \times 25$ kHz) to uniformly cover a 10-ppm proton spectrum ($\pm 2\pi \times 2.5$ kHz at 500 MHz). Peak power must be quadrupled to cut pulse lengths in half and yet keep $\omega_1 T = \pi$, so rectangular pulses are very wasteful of pulse power. In addition, residual excitation occurs very far outside the nominal pulse bandwidth. Gaussian pulses (*23*) eliminate the long frequency tails, at the expense of somewhat increased pulse length; Hermite pulses (*19, 24*) expand the completely excited bandwidth. At the opposite extreme, the asymmetric pulse shape of Fig. 4 provides a vastly larger completely excited bandwidth for the same peak power, but it is substantially longer. This longer pulse could present a problem if extremely narrowband excitation is desired; the pulse length could then be comparable to relaxation times.

$\pi/2$ Pulses. These pulses fall into two distinct categories: normal and self-refocused. $\pi/2$ Pulse shapes with envelopes similar to $(\sin \alpha T)/T$ excite a rectangular distribution (*12, 20, 25*). However, all such shapes exhibit phase roll, as do long rectangular pulses; this is a

Table 1. Bandwidths and lengths of different π pulse shapes with the same peak power, expressed in units of ω, the Rabi frequency (see text). Within the completely inverted region, magnetization starting at $+I_z$ ends up within 10° of $-I_z$. Outside of the completely uninverted region, magnetization starting at $+I_z$ ends up within 10° of $+I_z$. The expression describing the Hermite pulse is $(1 - 0.957t^2)\exp(-t^2)$, where t is time. The asymmetric pulse is shown in Fig. 4. Full-width at half-maximum, FWHM.

Pulse shape	Length	Completely inverted region	Bandwidth (FWHM)	Completely uninverted region
Rectangular	1.0	$< \pm 0.09\omega_1$	$\pm 0.80\omega_1$	$> \pm 11\omega_1$
Gaussian	2.0*	$< \pm 0.06\omega_1$	$\pm 0.63\omega_1$	$> \pm 1.6\omega_1$
Hermite	4.8*	$< \pm 0.15\omega_1$	$\pm 0.55\omega_1$	$> \pm 1.5\omega_1$
Asymmetric	8.0	$< \pm 0.45\omega_1$	$\pm 0.77\omega_1$	$> \pm 1.05\omega_1$

*These pulse shapes are assumed to be truncated at 5% of the peak amplitude.

consequence of linear response theory. Linear response predicts that the induced magnetization is proportional to the Fourier transform of the pulse. However, the point chosen as $T = 0$ for the Fourier transform has a dramatic effect (Fig. 5). A purely real transform is possible only if the pulse is symmetric and amplitude-modulated, and if $T = 0$ is chosen as the middle of the pulse. However, the FID cannot be detected until the pulse ends. This treatment gives an approximately linear phase shift with frequency, but such a correction is only exact if no lines overlap, and in most of the interesting cases spectral distortion ensues. In the extreme limit of a highly inhomogeneously broadened line, which is commonly encountered in optical spectroscopy or magnetic resonance imaging, the FID can disappear completely (*26*).

A subsequent intense π pulse can restore signal or remove this distortion, but a more selective approach is to design the excitation pulse itself to eliminate phase roll. This can be done with amplitude-modulated $3\pi/2$ pulses (*27, 28*) or with phase- and amplitude-modulated pulses (*28*). One specific self-refocused pulse shape and the effects of this pulse on 5 m*M* vitamin B_1 in water are shown in Fig. 6. These spectra are presented without phase correction. The triplet is excited without distortion, and the small residual signal from the huge water peak 2 ppm away shows good selectivity. We have demonstrated bandwidths as narrow as 15 Hz with 280-ms pulses (*28*).

NMR Applications: Solvent Suppression Sequences

The combination of a selective $+\pi/2$ pulse and a broadband $-\pi/2$ pulse can excite a broad region while missing a small region near resonance. This combination provides an approach for solvent suppression; the net effect of such "narrow reject" pulses in a complex sequence is to excite a normal-looking spectrum off resonance (*29*). In Fig. 7, 2D NMR spectra, again of vitamin B_1 in water, demonstrate the use of normal and narrow reject pulses (*30*). These spectra were taken with pulses that generated large phase roll, but more recent work (*31*) has combined the self-refocused pulses presented above with simple rectangular $-\pi/2$ pulses to produce solvent suppression without phase roll; these are called ERASER pulses. Most of the common solvent-suppression pulse sequences produce spectra with large phase or amplitude distortions (*32*).

ERASER pulse results on two samples of 4 m*M* bovine pancreatic trypsin inhibitor (BPTI) are shown in Fig. 8 (*31*). The spectrum of 4 m*M* BPTI in 80% H_2O after a single short rectangular pulse is shown in Fig. 8, A and B. The water peak dominates the spectrum, as it is 10,000 times more intense than the other peaks. The expanded spectrum is poorly resolved and has a rolling baseline. The spectrum of 4 m*M* BPTI in 98% D_2O (Fig. 8C), in which the water peak is greatly reduced, serves as a reference to which the suppressed spectrum can be compared. The ERASER pulse spectrum of 4 m*M* BPTI in 80% H_2O is shown in Fig. 8D. The features of this spectrum include an area of 2.5 ppm that is affected by the suppression sequence. The peaks outside this affected region are fully excited, as compared with Fig. 8C, and completely phased. This spectrum is presented with the same gain as the spectrum taken with a single hard pulse in Fig. 8B. Comparison of A and D in Fig. 8 yields the degree of suppression (~100:1). Exchangeable proton signals can be seen in Fig. 8D, but of course not in Fig. 8C.

I should note that combinations of several rectangular pulses with phase shifts (composite pulses) have been successfully applied in a wide variety of similar NMR applications (*33*), including solvent suppression (*34, 35*). A composite pulse can be viewed as a single constant amplitude waveform with discrete phase modulation, and as such has two principal disadvantages compared with continuous phase and amplitude modulation. Composite pulses are often extremely sensitive to radiation damping or relaxation effects because the total rotation (integrated area under the pulses) is large; relaxation or radiation damping creates a time-dependent fractional perturbation, and even a small effect can be cumulative. In addition, there is inevitably a large spurious excitation far from resonance because the phase discontinuities imply a broad Fourier transform.

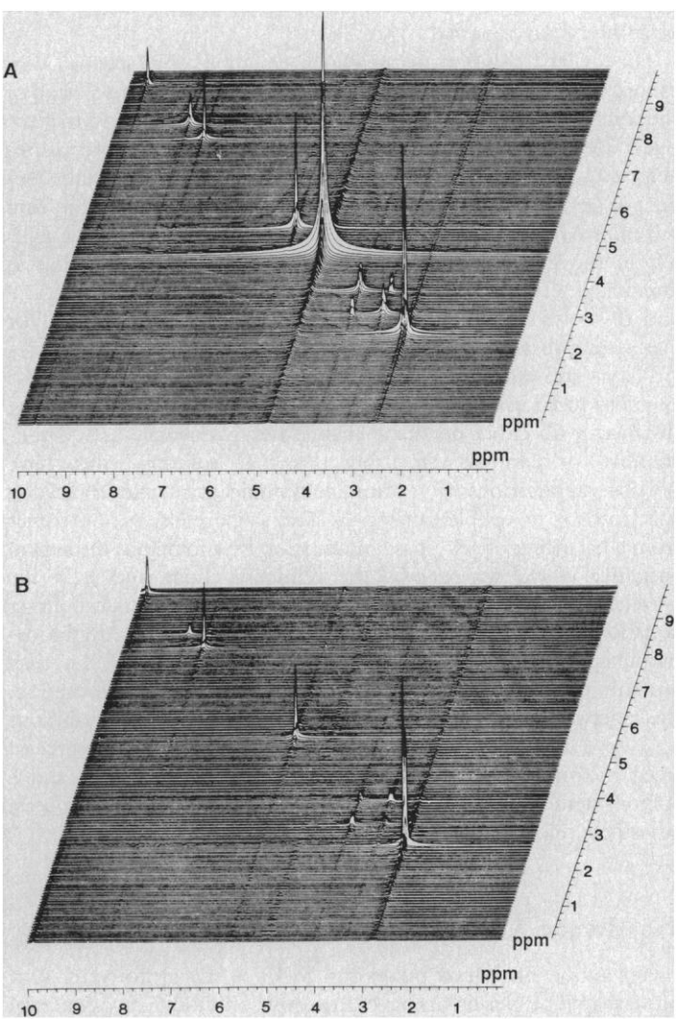

Fig. 7. Two-dimensional NMR spectra with (**A**) normal rectangular pulses and (**B**) solvent-suppressed pulses. [Reprinted with permission from *Chemical Physics Letters* (*30*)]

As a result, composite pulses cannot generate a clean narrowband excitation in a much broader spectrum. As might be expected, combinations of several shaped pulses with phase shifts partially overcome these problems (*36*).

Optical Applications: Optical Density Compensation and Soliton Generation

Pulse shapes can also be tailored for more demanding tasks, such as compensation for inhomogeneities or optical density effects. As an example, McCall and Hahn discovered in 1968 that a hyperbolic secant pulse of area 2π would propagate through an optically thick sample with no attenuation (*37*). This phenomenon of self-induced transparency has never proven particularly useful for spectroscopic applications: there is no attenuation because the pulse generates no net excitation. In addition, the pulse shape only remains unchanged if the area is exactly 2π. One is usually more interested in $\pi/2$ or π pulses; propagation effects on a hyperbolic secant π pulse are shown in Fig. 9. Pulse propagation effects considerably complicate the spectroscopy of mixed molecular crystals, as shown by Fayer and coworkers (*38*); photon echo decays have time constants that explicitly depend on the optical density, even if the concentration of absorbers is kept constant (for example, only the crystal length is changed). This dependence occurs qualitatively because the shape and amplitude of the echo is distorted by propagation, and changes as the interpulse delay is varied.

The analytic solution of the Bloch equations for $(\text{sech}\ \alpha T)^{1+5i}$ cannot be extended to optically thick samples. Computer solution of the coupled Maxwell-Bloch equations for this shape showed that the pulse does not substantially reshape or lengthen as it propagates (Fig. 10), which means that the inversion profile is nearly independent of optical density (*39*). This phenomenon is very different from self-induced transparency, which works in part because no energy is left in the molecules. This pulse excites everything and thus is attenuated, yet it produces a constant result. Comparison of Figs. 9 and 10 shows that pulse shaping is an extremely important tool for eliminating distortions from optical density effects.

Phase- and amplitude-modulated soliton laser pulses have also been produced in optical fibers. Such pulses can propagate over long distances with either no shape change ("fundamental" or "$N = 1$" solitons) or periodic refocusing ("$N > 1$" solitons); they have possible applications to optical communications and molecular spectroscopy in coupled materials. The shape conservation comes from a balancing of self-phase modulation by anomalous dispersion (negative $dn/d\lambda$, where n is the refractive index and λ is the wavelength), and is calculated by solving the nonlinear Schrödinger equation that describes pulse propagation in a fiber. Amplitude-modulated solitons had been demonstrated previously (*40*), but they are only possible over a limited range of wavelengths; in addition, the exact soliton amplitude and the period of the soliton solutions for $N > 1$ are dictated by materials parameters. The extra degree of freedom from phase modulation lets us generate $N = 1$, 2, and 3 solitons with the same (user-adjustable) peak power, and with user-adjustable refocusing periods (*41*) (Fig. 11).

Hardware Modifications for Pulse Shaping

Generation of shaped pulses for NMR is straightforward. Our pulse-shaping experiments have been done on modified commercial NMR spectrometers with proton resonance frequencies from 90 to 500 MHz. The spectrometer produces its normal rectangular pulses, which are intercepted just before the final output amplifier (*12*).

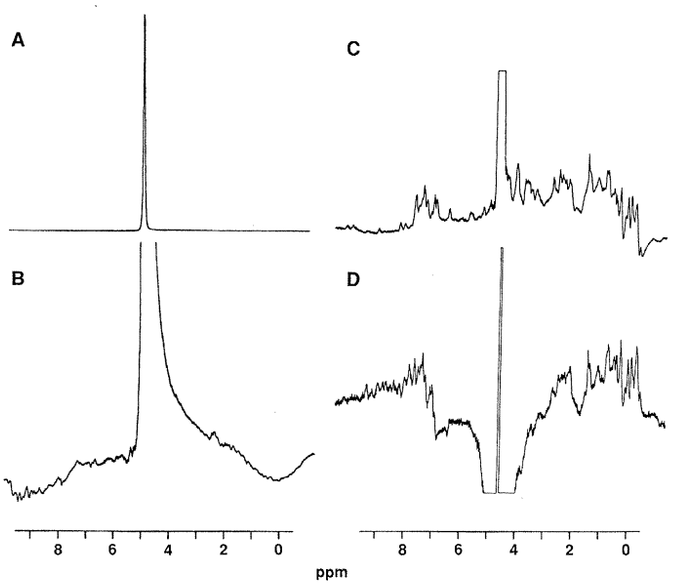

Fig. 8. NMR spectra of 4 m*M* solutions of BPTI. (**A**) Normal spectrum in 80% H_2O. (**B**) Vertical scale expansion of the spectrum in (A). (**C**) Normal spectrum in 98% D_2O. (**D**) Spectrum from a self-refocused solvent suppression "ERASER pulse" in 80% H_2O. No amplitude or phase corrections have been applied to any of these spectra. [Reprinted with permission from *Journal of Magnetic Resonance* (*31*)]

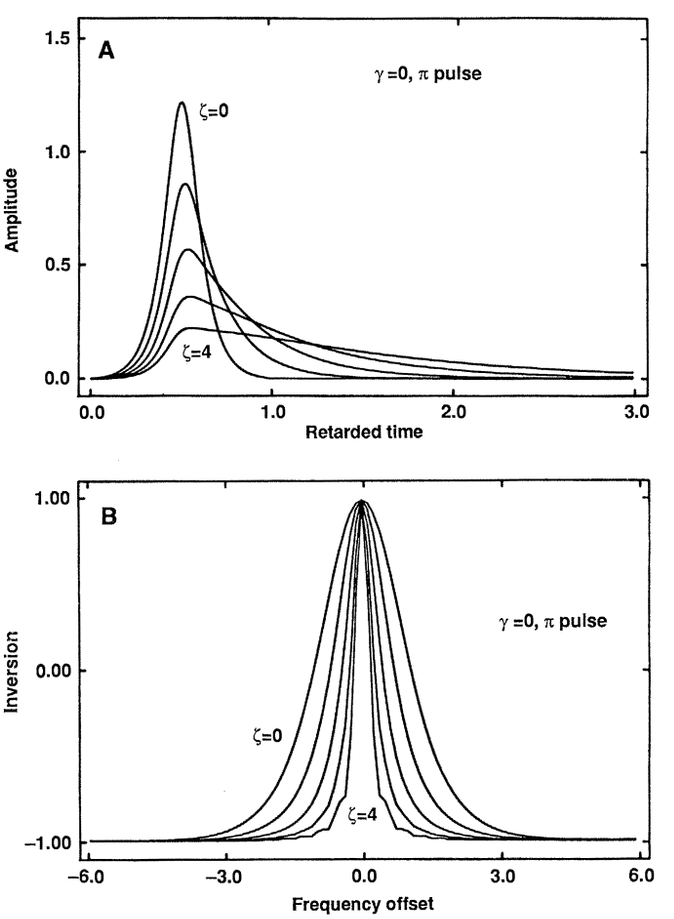

Fig. 9. (**A**) Pulse envelope and (**B**) inversion profile for an unmodulated sech αT pulse with area π as a function of distance into an optically thick sample. The parameter ζ is the number of Beer's lengths into the sample, and ranges from 0 to 4. [Reprinted with permission from *Physical Review A* (*39*)]

Shaped pulses are generated by commercially available boards that are installed into an IBM PC, giving 12-bit, 2048-point approximations to any desired pulse envelope with 200-ns resolution. The rest of the circuitry simply imposes the envelope on the RF, after which the shaped pulses are amplified and sent to the probe. The power advantages of pulse shaping allow the use of a 2-watt (linear) amplifier as the largest power source in any of the experiments presented here.

Generation of shaped laser pulses on an experimentally useful time scale (10^{-13} to 10^{-9} s) is not as straightforward, but also not as difficult as might be expected. For example, the shapes in Fig. 11 were each generated as an envelope and a phase function by a programmable GaAs FET-based microwave pulse generator (*42*), and passed to homebuilt waveguide electrooptic modulators with 10 to 20 GHz bandwidth (*41, 42*) (Fig. 12). Devices with nearly comparable performance are now commercially available. Visible shaped pulses can be amplified to megawatt peak powers (*42*) and can generate sequences of shaped pulses with complete phase control (*8*).

A method has recently been developed for producing voltage-programmable, arbitrarily shaped laser pulses with roughly 100-fs resolution (*43*) by modifying the widely used technique of fiber-grating compression (*44*). A relatively long (picosecond) pulse is passed through a single mode optical fiber, which "chirps" the pulse (generates a linear frequency sweep with time) and temporally broadens it. In the normal application, a grating pair then provides a different path length for the different colors in the pulse, and the net effect can be a substantial shortening (to as little as 6 fs) (*45*). In my laboratory the pulse was tailored (after the fiber, where it is temporally dispersed) with a high bandwidth (19.5-GHz) waveguide intensity modulator. Optical pulses with $(\sin x)/x$ and square envelopes were synthesized to demonstrate the technique (Fig. 13). Recent developments of modulators with 100-GHz bandwidth (3-ps risetime) can make this technique even more versatile (*46*).

An alternative approach is to insert custom-fabricated phase and amplitude masks between the diffraction gratings (*47*). This approach effectively tailors the Fourier transform of the pulse; the choice between these techniques at this point depends on the importance of programmability and the complexity of the desired envelope versus the complexity of its Fourier transform. However, both approaches are certain to continue to evolve.

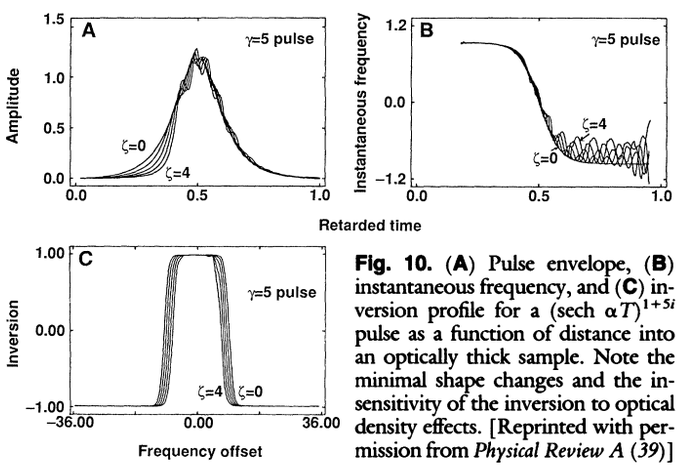

Fig. 10. (**A**) Pulse envelope, (**B**) instantaneous frequency, and (**C**) inversion profile for a (sech $\alpha T)^{1+5i}$ pulse as a function of distance into an optically thick sample. Note the minimal shape changes and the insensitivity of the inversion to optical density effects. [Reprinted with permission from *Physical Review A* (*39*)]

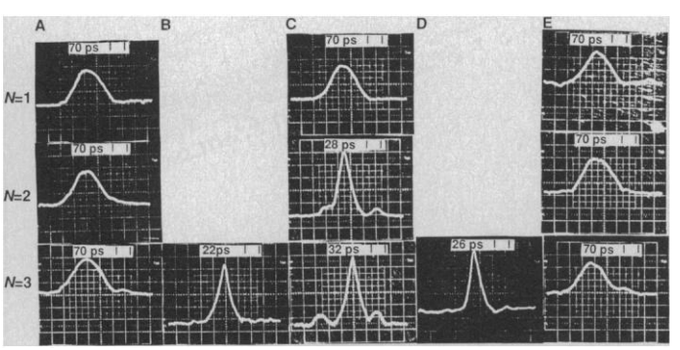

Fig. 11. Autocorrelation functions of phase- and amplitude-modulated pulses after propagation lengths of (**A**) 0, (**B**) 200, (**C**) 400, (**D**) 600, and (**E**) 800 m after propagation through an optical fiber. The predicted periodicity, compression, and structure are observed experimentally. The phase modulation is substantial (the $N = 3$ soliton ranges from $-\pi/2$ to π with four oscillations), but it reduces sensitivity to amplitude fluctuations and permits user-adjustable peak power and refocusing period. [Reprinted with permission from *Physical Review Letters* (*41*)]

Conclusions

In conclusion, pulse shaping provides an extra degree of freedom that has already been shown to be helpful in a wide variety of experimental contexts. Examples have been restricted here to well-understood applications. Current NMR frontiers include shaped pulse sequences to give larger uniformly excited bandwidths for spin-1 powder patterns; shapes designed to optimize performance of multiple pulse sequences for dipolar coupled spins; and shapes that compensate for radiation damping. Optical frontiers include applications of two (sech $\alpha T)^{1+5i}$ pulses with different colors to make quantitative population transfers to vibrationally excited levels of the ground electronic state. There has also been recent speculation that shaped laser pulses (*48*) or a well-defined phase relation between multiple lasers (*49*) can promote state-selective chemistry. Thus the availability of the technology and clear advantages in a

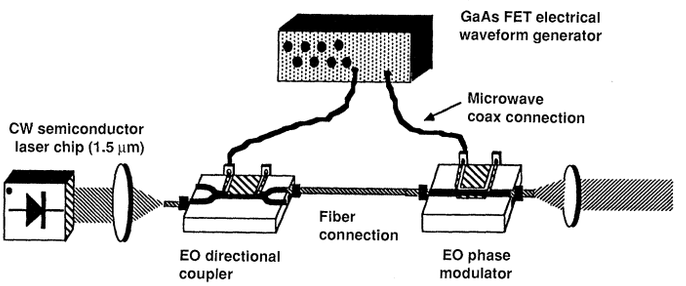

Fig. 12. Experimental apparatus for generating the phase- and amplitude-modulated pulses shown in Fig. 11. [Reprinted with permission from *Physical Review Letters* (*41*)]

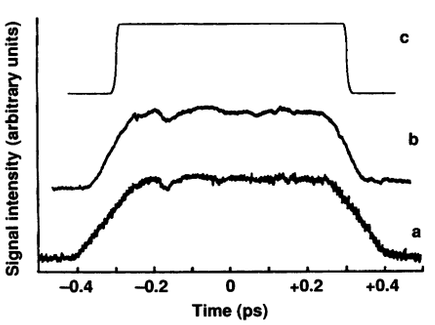

Fig. 13 (**a**) Experimental cross-correlation function (cross-correlated with a 180-fs pulse) of a synthesized rectangular laser pulse. (**b**) Cross-correlation function with the shorter pulse deconvolved. (**c**) Target shape. This is one example of voltage-programmable pulse shaping with <100-fs resolution; rectangular pulses with lengths from 600 to 1300 fs and $(\sin x)/x$ pulses with comparable resolution have been produced as well. [Reprinted with permission from *Applied Physics Letters* (*44*)]

variety of applications imply that shaped pulses are likely to become broadly and routinely applied in the near future.

REFERENCES AND NOTES

1. R. R. Ernst, G. Bodenhausen, A. Wokaun, *Principles of Nuclear Magnetic Resonance in One and Two Dimensions* (Oxford Univ. Press, London, 1987).
2. M. D. Levenson and S. S. Kano, *Introduction to Nonlinear Laser Spectroscopy* (Academic Press, New York, 1988).
3. R. Beach and S. R. Hartmann, *Phys. Rev. Lett.* **53**, 663 (1984); N. Morita and Y. Tajima, *Phys. Rev. A* **30**, 2525 (1984); S. Asaka, H. Nakatsuka, M. Fujiwara, M. Matsuoka, *ibid.* **29**, 2286 (1984); H. Nakatsuka, M. Tomita, M. Fujiwara, S. Asaka, *Opt. Commun.* **52**, 150 (1984).
4. T. E. Orlowski and A. H. Zewail, *J. Chem. Phys.* **70**, 1390 (1979); W. S. Warren and A. H. Zewail, *ibid.* **75**, 5956 (1981).
5. W. S. Warren and A. H. Zewail, *ibid.* **78**, 2279 (1983).
6. E. T. Sleva, I. M. Xavier, A. H. Zewail, *J. Opt. Soc. Am.* **B3**, 483 (1986).
7. Y. S. Bai, A. G. Yodh, T. W. Mossberg, *Phys. Rev. Lett.* **55**, 1277 (1985).
8. W. S. Warren and M. Haner, in *Atomic and Molecular Processes with Short Intense Laser Pulses*, A. Bandrauk, Ed. (Plenum, New York, 1988), p. 1; F. Spano, M. Haner, W. S. Warren, *Chem. Phys. Lett.* **135**, 97 (1987).
9. A. Mukherjee, N. Mukherjee, J.-C. Diels, G. Arzumanyan, *Ultrafast Phenomena V*, G. Fleming and A. Siegman, Eds. (Springer, Berlin, 1986), p. 266.
10. W. S. Warren and A. H. Zewail, *J. Chem. Phys.* **78**, 3583 (1983); J. C. Diels and S. Besnainou, *ibid.* **85**, 6347 (1986).
11. W. S. Warren and A. H. Zewail, *ibid.* **78**, 2298 (1983).
12. W. S. Warren and M. S. Silver, *Adv. Magn. Reson.* **12**, 248 (1988).
13. I. I. Rabi, *Phys. Rev.* **51**, 652 (1937).
14. L. Allen and J. H. Eberly, *Optical Resonance and Two-Level Atoms* (Wiley, New York, 1975); F. T. Hioe, *Phys. Rev. A* **30**, 2100 (1984); M. S. Silver, R. I. Joseph, D. I. Hoult, *ibid.* **31**, 2753 (1985); J. Baum, R. Tycko, A. Pines, *ibid.* **32**, 3435 (1985).
15. W. S. Warren, *Soc. Photo. Opto. Instrum. Eng.* **742**, 42 (1987).
16. C. P. Lin, J. Bates, J. Mayer, W. S. Warren, *J. Chem. Phys.* **86**, 3750 (1987).
17. A. Hasenfeld, S. Hammes, W. S. Warren, *Phys. Rev. A*, in press.
18. F. A. Grünbaum and A. Hasenfeld, *Inverse Prb.* **2**, 75 (1986); A. Hasenfeld, *J. Magn. Reson.* **72**, 509 (1987).
19. W. S. Warren, *J. Chem. Phys.* **81**, 5437 (1984); M. McCoy and W. S. Warren, *J. Magn. Reson.* **65**, 178 (1985).
20. J. Murdoch, A. Lent, M. Kritzer, *J. Magn. Reson.* **74**, 226 (1987).
21. S. Connolly, D. Nishimura, A. Macovski, *IEEE Trans. Med. Imaging* **M15**, 106 (1986); D. J. Lurie, *Magn. Reson. Imaging* **3**, 235 (1985); F. Loaiza *et al.*, *Health Care Instrum.* **1**, 188 (1986); R. R. Edelman, D. Atkinson, M. Silver, F. Loaiza, W. S. Warren, *J. Radiol.* **166**, 231 (1988).
22. F. Loaiza, thesis, Princeton University, Princeton, NJ (1988).
23. C. Bauer, R. Freeman, T. Frankiel, J. Keeler, A. J. Shaka, *J. Magn. Reson.* **58**, 442 (1984); D. E. Cooper and M. D. Fayer, *Chem. Phys. Lett.* **67**, 41 (1979).
24. M. A. Banash and W. S. Warren, *Laser Chem.* **6**, 47 (1986).
25. M. S. Silver, R. I. Joseph, D. I. Hoult, *J. Magn. Reson.* **59**, 347 (1984).
26. F. Loaiza, M. McCoy, M. Levitt, M. S. Silver, W. S. Warren, *ibid.* 76, 504 (1988); D. Hoult, *ibid.* **35**, 69 (1979).
27. J. T. Ngo and P. G. Morris, *Biochem. Soc. Trans.* **14**, 1271 (1986).
28. F. Loaiza, M. McCoy, S. Hammes, W. S. Warren, *J. Magn. Reson.* 77, 175 (1988).
29. J. Gutow, M. McCoy, F. Spano, W. S. Warren, *Phys. Rev. Lett.* **55**, 1090 (1985).
30. M. McCoy and W. S. Warren, *Chem. Phys. Lett.* **133**, 165 (1987).
31. M. McCoy, F. Loaiza, K. Valentine, W. S. Warren, *J. Magn. Reson.*, in press.
32. A. G. Redfield, S. D. Kunz, E. K. Ralph, *ibid.* **19**, 114 (1975); P. J. Hore, *ibid.* **55**, 283 (1983); *ibid.* **56**, 535 (1984); P. Plateau and M. Gueron, *J. Am. Chem. Soc.* **104**, 7310 (1982); Z. Starcuk and V. Sklenar, *J. Magn. Reson.* **61**, 567 (1985); *ibid.* **66**, 391 (1986).
33. M. Levitt, *Prog. Nucl. Magn. Reson. Spectrosc.* **18**, 61 (1986).
34. M. H. Levitt and M. F. Roberts, *J. Magn. Reson.* 71, 576 (1987).
35. M. von Kienlin, M. Decorps, J. P. Albrand, M. F. Foray, P. Blondet, *ibid.* **76**, 169 (1988).
36. W. S. Warren, J. Bates, M. McCoy, M. Navratil, L. Mueller, *J. Opt. Sci. Am.* **B3**, 488 (1986).
37. S. L. McCall and E. L. Hahn, *Phys. Rev.* **183**, 457 (1969).
38. R. W. Olson, H. W. H. Lee, F. G. Patterson, M. D. Fayer, *J. Chem. Phys.* 76, 31 (1982).
39. F. Spano and W. S. Warren, *Phys. Rev. A* **37**, 1013 (1988).
40. L. F. Mollenauer, R. H. Stolen, J. P. Gordon, *Phys. Rev. Lett.* **45**, 1095 (1980); L. F. Mollenauer and R. H. Stolen, *Opt. Lett.* **9**, 13 (1984).
41. M. Haner and W. S. Warren, *Phys. Rev. Lett.*, in press.
42. ———, *Appl. Opt.* **26**, 3687 (1987); M. Haner, F. Spano, W. S. Warren, *Ultrafast Phenomena V*, G. Fleming and A. Siegman, Eds. (Springer, Berlin, 1986), p. 514.
43. M. Haner and W. S. Warren, *Appl. Phys. Lett.* **52**, 1458 (1988).
44. C. V. Shank, R. L. Fork, R. Yen, R. H. Stolen, W. J. Tomlinson, *ibid.* **40**, 761 (1982).
45. R. L. Fork, C. H. Brito Cruz, P. C. Becker, C. V. Shank, *Opt. Lett.* **12**, 483 (1987).
46. J. Ness, in *Conference on Lasers and Electro-Optics Technical Digest Series 1988* (Optical Society of America, Washington, DC, 1988), vol. 7, p. 487.
47. A. M. Weiner, J. P. Heritage, R. N. Thurston, *Opt. Lett.* **11**, 153 (1986); *ibid.* **10**, 609 (1985).
48. H. Rabitz, in *Atomic and Molecular Processes with Short Intense Laser Pulses*, A. Bandrauk, Ed. (Plenum, New York, 1988).
49. P. Brumer and M. Shapiro, *Chem. Phys. Lett.* **126**, 541 (1986).

50. NMR work was supported by the National Institutes of Health under grant GM 35253 BBCB and by the National Science Foundation under grant CHE-8502199. Optical work was supported by the National Science Foundation under grant CHE-8719545 and by DARPA (administered by NSWC). I also wish to thank the reviewers for useful comments.